Towards 5G: Performance Evaluation 60 GHz UWB OFDM Communications under both Channel and RF impairments.

Rodolfo Gomes[a,b], Akram Hammoudeh[b], Rafael F. S. Caldeirinha[a,b,*], Zaid Al-Daher[a], Telmo Fernandes[a,b], Joao Reis[a,b]

[a] *University of South Wales, School of Engineering, Treforest, United Kingdom.*
[b] *Instituto de Telecomunicações (DL-IT), ESTG, Polytechnic Institute of Leiria, Portugal.*

Abstract

Detailed analysis on the impact of RF and channel impairments on the performance of Ultra-Wideband (UWB) wireless Orthogonal Frequency Division Multiplexing (OFDM) systems based on the IEEE 802.15.3c standard, for high data-rate applications using the 60 GHz millimetre frequency band is presented in this paper. This frequency band, due to the large available bandwidth is very attractive for future and 5G wireless communication systems. The usage of OFDM at millimetre-wave (mmWaves) frequencies is severely affected by non-linearities of the Radio Frequency (RF) front-ends. The impact of impairments is evaluated, in terms of some of the most important key performance indicators, including spectral efficiency, power efficiency, required coding overhead and system complexity, Out-Of-Band Emissions (OOBEs), Bit Error Rate (BER) target and Peak Signal-to-Noise Ratio (PSNR). Additionally, joint distortion effects of coexisting Phase-Noise (PN), mixer IQ imbalances and Power Amplifier (PA) non-linearities, on the performance degradation of a mmWave radio transceiver, combined with various multipath fading channels, are investigated. Subsequently, the power efficiency of the system is evaluated by estimating values of the PA Output-Power-Backoff (OBO) needed to meet the requirements for the Transmit Spectrum Mask (TSM) and BER target. Finally, a comparison

*Corresponding author
Email address: rafael.caldeirinha@ipleiria.pt (Rafael F. S. Caldeirinha)

of the system overall performance between uncoded and coded OFDM systems combined with Quadrature Amplitude Modulations (QAMs) (16 and 64 QAM) and its maximum operable range are evaluated by transmitting a Full HD uncompressed video frame under five different RF impairment conditions over a typical LOS kiosk 60 GHz IEEE channel model.

Keywords: `Communication system performance, Channel coding, Fading channels, Millimetre wave communication, Millimetre wave amplifiers, Phase noise.`

2010 MSC: 00-01, 99-00

---

1. Introduction

Radio communication systems at 60 GHz have recently attracted a great deal of interest for future 5G wireless networks, due to the wide available bandwidths to accommodate multi-gigabit transmission rates and to the possibility of highly integrated transceivers at these frequencies. The IEEE 802.15.3c [1], created by Task Group 3c [2], is earmarked as the Wireless Personal Area Network (WPAN) standard for the band 57-66 GHz in Europe [3], with expected data rate targets ranging between 2 and 5 Gb/s. This standard details the implementation of a 60 GHz communication system from a physical layer (PHY) design point of view, considering different target applications or usage models [4].

Millimetre-wave communications benefit from a large unlicensed bandwidth, which enables new wireless applications such as High Definition Multimedia Interface (HDMI) for uncompressed video/audio streaming and multi-gigabit file data transfer. The relatively high free-space signal path loss and high attenuation by walls, furniture and other objects, simplify the frequency reuse factor over small distances [5]. The wavelength in free-space is around 5 mm at 60 GHz, which highly reduces the size of the devices. However, there are some drawbacks that must be taken into account at mmWave frequencies, which are mostly related to the non-linearities of the RF front-ends [6]. A signal conversion from baseband to 60 GHz introduces a relatively higher PN in comparison

to lower frequencies [7]. In [8], it is also demonstrated that phase noise floor, presented in the oscillators, is significantly increased at mmWave frequencies. For instance, if the desired frequency at the input of the mixer is f and the original frequency from the reference source is f_o, the final phase noise will be $20\log_{10}(f/f_o)$ dB above the original level. In addition, the upconversion of baseband signals at the transmitter and their down conversion back to baseband at the receiver, using IQ mixers, causes the RF front-ends to induce several critical non-idealities affecting both transmitted and received radio signals. Such non-linearities, including Phase-Noise (PN), IQ imbalances and Power Amplifier (PA) non-linear distortions, should be taken into account in radio design and link quality.

Despite the existence of a large number of articles addressing RF impairments at 60 GHz published in literature, to the authors' knowledge, none of them present a comprehensive critical survey analysis of the performance of Orthogonal Frequency Division Multiplexing (OFDM) under RF and channel impairments, leading in loss of subcarrier orthogonality and hence degradation in system performance. For example, in [9], the IQ imbalances are not considered and only low modulation orders are used. In [10] and [11], only the impact of a typical PA on the transmitter side is considered. Moreover, in [12, 13, 14, 15], the comparison is performed without considering the proposed standard specifications [1] and the appropriate RF impairment models for 60 GHz communication systems, reported in [16] and [17]. Finally in [8], only simulation results of error vector magnitude vs. difference phase noise floor levels are assessed targeting the E-band. Also in [18], semi-analytical methods to estimate the error-rate for uncoded OFDM systems are proposed, considering non-Gaussian distributions for the joint interference of RF impairments in contrast to taking into account realistic models at mmWave spectrum, as presented in this paper. Additionally, PA non-linearities are not considered in the work presented in [18].

Following a preliminary study done by the authors [19], this paper presents an extensive study on the impact that both RF and channel impairments have

on the performance of OFDM wireless communication systems at 60 GHz. The authors intend to provide a realistic channel and RF impairment models for mmWave spectrum, which are essential for system assessment, radio planning, and link budget analysis for giga-bit per second wireless applications, such as uncompressed video streaming. An end-to-end simulation framework based on the IEEE 802.15.3c standard [1] is developed, which can be used to predict system performance for future radio networks. According to [20, 21], to compensate for the expected growth of users and the consequent overloading of the frequency spectrum that will caused by 5G, the use of the unlicensed mmWave spectrum (especially the 60 GHz) is very likely. This band is due to be standardized for 5G applications by 2020.

Firstly, the system performance is characterized under an Additive White Gaussian noise (AWGN) channel in order to determine the effects of RF impairments in the absence of other factors such as multipath propagation. The models used for RF impairments are similar to those proposed in [16] and [17] for the PN, IQ imbalances and PA non-linearities. Two realistic power amplifier models of different technologies (CMOS and GaAs) are considered. For each model, the PA Output-Power-Backoff (OBO) needed to meet the requirements for the Transmit Spectrum Mask (TSM) [1] and BER target is presented. Secondly, the overall OFDM (both uncoded and coded) system performance, is evaluated taking into account both RF and channel impairments, by transmitting a Full High Definition (HD) uncompressed video frame under five different impairment conditions, as detailed in section 5. Finally, Forward Error Correction (FEC) codes, in particular, Reed Solomon (RS) and Low-Density Parity-Check (LDPC) codes, aimed at reducing the effects inherent from the RF front-ends and from the radio propagation channel, are implemented. As metrics, Bit Error Rate (BER), Out-Of-Band Emissions (OOBEs) and maximum system range are used for performance assessment. Peak Signal-to-Noise Ratio (PSNR) is used to assess the received quality of service in an uncompressed video streaming application (UM1 [4]) using Equal Error Protection (EEP). For millimetre-wave (mmWaves), in general, a link with a dominant Line-of-sight (LOS) is required

to support higher throughput and higher range of operation [4]. For example, the data rate requirement to transmit a Full HD video content at a frame rate of 90 Hz and 30 bits per channel per pixel, which are the expected revised specifications to improve the quality of HDTV [22], is 5.6 Gbps. The IEEE CM9 standard model [2], typically for indoor LOS Kiosk environment, is employed in the analysis presented in this paper.

The paper is organized as follows. Section 2, presents the RF impairment models for PN, IQ imbalances and PA non-linearities. Section 3, details implementation of both coded and uncoded OFDM system modelling. Section 4, provides results of the OFDM performance degradation due to each RF impairment, together with link-budget analysis. Section 5, presents the OFDM BER and PSNR simulation results for a typical RF front-end architecture considering a number of different impairment scenarios. Finally, the main conclusions are drawn in section 6.

2. RF impairment modelling at 60 GHz

Behavioural modelling and simulation of non-linear systems play an important role in the evaluation of an overall communication system design and performance. In this section, modelling of RF impairments is presented.

2.1. Phase Noise and IQ Imbalances

In a typical radio communication systems operating at the sub-6 GHz band, the IQ mixing and upconversion/downconversion stages are being replaced by software implementations, making the system less susceptible to hardware imperfections and non-linearities. However, at 60 GHz, performing upconversion/downconversion by digital signal processing algorithms is impracticable, since a minimum sampling rate of 120 GS/s would be required to comply with the Nyquist criteria. Therefore, for such high frequencies, RF conversions are preferably implemented in hardware. Oscillators for the RF conversions and IQ mixers for the Quadrature Amplitude Modulations (QAMs), and such hardware imperfections should be taken into account in a mm-Wave system design. For

example, it is very unlikely to have two oscillators operating at the exact same carrier frequency and thus distortion in the OFDM signal due to this effect is always present, causing Inter-Carrier Interference (ICI) and Common Phase Rotation (CPR) [12], also known as phase-noise. By performing an interpolation of the data obtained from measurements at 60 GHz it has been demonstrated that PN can be modelled as a high-pass filter [16], given by:

$$PSD(f) = PSD(0)\frac{[1+(f/f_z)^2]}{[1+(f/f_p)^2]}, \tag{1}$$

where, $PSD(0)$ is the low frequency phase noise, f_p is the pole filter frequency and f_z is the zero filter frequency. Thus, by considering different values of $PSD(0)$, the PN spectral density model can be adjusted for different competing Integrated Circuit (IC) technologies, such as 0.25 μm/0.13 μm Complementary Metal-Oxide-Semiconductor (CMOS) Voltage-Controlled Oscillators (VCOs), 0.25 μm BipolarCMOS (BiCMOS) Phase-Locked Loop (PLL) with frequency tripler and a Silicon-germanium (SiGe) PLL, as is depicted in Fig. 1 according to [16].

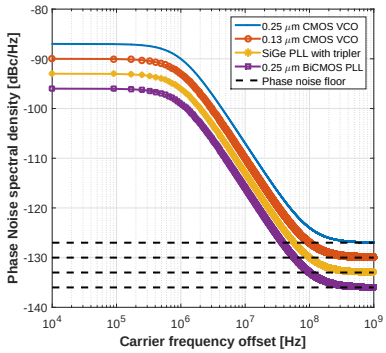

Figure 1: Power spectral density for different VCO and PLL CMOS/SiGe IC technologies.

IQ imbalances are described by the phase and amplitude offset between I and Q branches, in quadrature amplitude modulators/demodulators. The complex baseband output signal, which suffers this mismatch, can be defined by [22]:

$$y(t) = [\cos(\Delta\phi) + j\Delta g \sin(\Delta\phi)]x(t) +$$

$$[\Delta g \cos(\Delta\phi) - j \sin(\Delta\phi)]x^*(t), \tag{2}$$

where, $x(t)$ is the input signal, $x^*(t)$ is its complex conjugate and, Δg and $\Delta\phi$ are the gain and phase mismatches, respectively. From (2), it can be seen that $x(t)$ is interfered with its image signal, $x(t)^*$, causing attenuation and a rotation of the desired signal.

2.2. Power Amplifier

Radio Signals are subject to both amplitude and phase distortions when passing a power amplifier. Such distortions are visible not only in the signal bandwidth but also as out of band emissions.

For a generic amplifier stage, the input signal $x(t)$, given by $x(t) = A(t)\cos[2\pi f_c t + \theta(t)]$, is amplified and characterized by $y(t) = G[A(t)]\cos(2\pi f_c t + \theta(t) + \psi[A(t)])$, where $G[A(t)]$ is the amplitude distortion, also known as amplitude modulation to amplitude modulation (AM-AM) and $\psi[A(t)]$ is the amplitude modulation to phase modulation (AM-PM). In [16], the Rapp model for AM-AM [23] has been used and modified to extend it to include the AM-PM effects. Spectral regrowth and distortions on the constellation scheme of a 60 GHz PA can be therefore modelled by [16]:

$$F_{AM-AM}(|x[n]|) = \frac{G|x[n]|}{(1 + (\frac{|x[n]|}{V_{sat}})^{2s})^{\frac{1}{2s}}}, \tag{3}$$

$$F_{AM-PM}(|x[n]|) = \frac{\alpha|x[n]|^{q_1}}{(1 + (\frac{|x[n]|}{B})^{q_2})}, \tag{4}$$

where G is the voltage gain of the PA, V_{sat} is the saturation voltage level, $|x[n]|$ is the input voltage level, s ($s > 0$) is the smoothness factor that controls the transition from the linear zone to the saturation zone, α, B and q are constants and representing fitting parameters.

In order to mitigate the distortion introduced by the power amplifier, its quiescent operating point should be set to operate in the linear region, otherwise out-of-band emissions (intermodulation products) will appear in the output signal spectrum. And thus, leading to a high Adjacent Channel Interference (ACI)

and ISI, contributing to the degradation of the transmitted signal. In addition, if the input signal envelope is not constant, the operation point of the PA will vary. In practice to avoid (or at least to reduce) the effects of non-linearities, the PA should be operated at a given OBO set to a specific level keeping the signal within the linear region, at the expense of less power efficiency.

The PA OBO is given by:

$$OBO = 10 \log 10(\frac{P_{sat}}{P_{out}}), \tag{5}$$

where, P_{out} is the average output power from the PA and P_{sat} corresponds to the maximum output power (saturating power). The OBO parameter is highly important, since OFDM systems are characterized by large signal amplitude fluctuations, which make it susceptible to system non-linearities. Such amplitude fluctuations are characterized by the PAPR of the signal. The PAPR measures instantaneous power compared to the average power of the OFDM symbols and for the discrete-time signal is expressed as:

$$PAPR(x[n]) = max_{0 \leq n \leq N_c - 1} \frac{|x[n]|^2}{E[|x[n]|^2]}, \tag{6}$$

where, $|x[n]|^2$ is the maximum instantaneous power, $E[.]$ is the average power and N_c is the number of the subcarrier per OFDM signal.

The Power Added Efficiency (PAE), denoted by η, is defined as the ratio of the amplified output signal power to the DC power supplied to the amplifier, which is expressed by:

$$\eta = \frac{P_{out} - P_{in}}{P_{DC}}, \tag{7}$$

where, P_{in} is the input power, P_{out} is the desired output power in the band of interest and P_{DC} is the DC input power.

The values characterizing the PA non-linearities, given in Table 1, for two competing IC technologies have been calculated by fitting data obtained from 60 GHz measurements on Gallium Arsenide (GaAs) pHEMT [17] and a 65 nm CMOS [24] to the models presented in (3) and (4). The power and voltage characteristics for both GaAs and CMOS PA models, together with the AM/AM transfer functions assuming a 50Ω input impedance, are given in Fig. 2a and

Table 1: Modelling parameters for the considered PA models.

Model	**Gain**	V_{sat}**[V]**	**s**	α	**B**	q_1	q_2
GaAs	19	1.98	0.81	-48000	0.123	3.8	3.7
CMOS	4.65	0.82	0.81	2560	0.114	2.4	2.3

Fig. 2b, respectively. In addition, the AM/PM characteristics of the amplifiers are depicted in Fig. 2c.

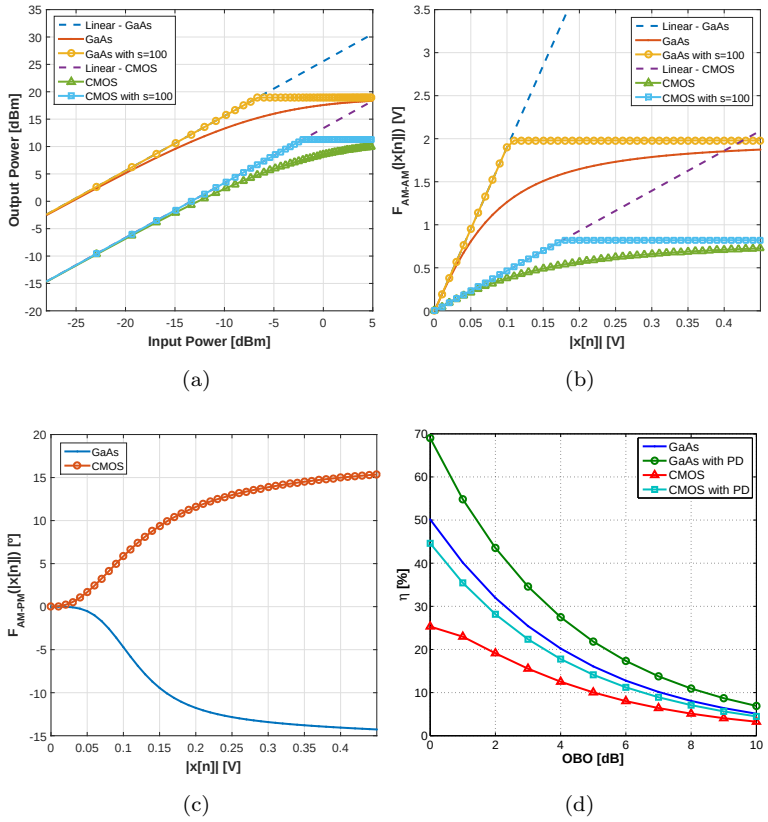

Figure 2: PA characteristic curves of: AM/AM for (a) power and (b) voltage, (c) AM/PM in function of input voltage and (d) relation between PAE and OBO for GaAs and CMOS model amplifiers.

According to Fig. 2b), the voltage AM/AM curves exhibit a linear char-

acteristic for low input signal amplitudes, followed by a transition towards a constant saturated output. Additionally, it is evident that as the smoothness function becomes increasingly large ($s \to \infty$), the Rapp model converges towards a perfect Pre-Distortion (PD) technique. This is verified for both PA technologies and observed when $s = 100$.

The PA is the main power consuming device in a transceiver. Therefore it is important to operate it close to its saturation point. However, as it was cited above, distortions occur due to the signal high PAPR., and a trade-off between the PA OBO and efficiency must be taken into account. This trade-off is shown in Fig. 2d for both PA models, with and without employing PD. Results for the CMOS PA have been obtained with the DC power value of 14.59 dBm [24]. As no DC power value is reported in literature for GaAs PA, its value was interpolated from reference (blue curve), assuming OBO = 0 and $\eta = 50\%$. Fig. 2d shows that the GaAs PA has much higher PAE than the CMOS model and when employing a PD technique, the PAE increases significantly, i.e. CMOS PA has an increased PAE of about 20%.

3. mmWave System Model based on IEEE 802.15.3c standard

The presented OFDM system model was developed based on the IEEE 802.15.3c standard [1] and is illustrated in Fig. 3, with the physical operating parameters given in Table 2 [1], for both 16 QAM and 64 QAM. Their constellations are mapped to Gray-code and their output values are obtained by multiplying the constellation points with a normalization factor. The FEC codes, bit and tone interleaver blocks are directly provided by the standard. In order to shape the OFDM signal Power Spectral Density (PSD) the subcarriers are allocated into the IFFT according to [1]. The wireless channel employed is based on the IEEE model proposed in [2]. The received signal, $y(t)$, after being processed using a K- point FFT, is converted into its frequency domain, $Y(k)$.

Table 2: Main parameters considered in the design of uncoded OFDM system based on IEEE 802.15.3c standard.

Parameter	**Value**
FFT size block (N_{fft})	512
Cyclic prefix (N_{cp})	64 samples
Sampling rate	2640 MHz
Nominal Used Bandwidth	1815 MHz
Sub-carrier bandwidth	5.15 MHz
Cyclic prefix time (T_{cp})	24.24 ns
Symbol time	218.18 ns
Throughput	6.2 Gbps

The received OFDM signal, Y_l, is given by:

$$Y_l(k) = H_l(k).X_l(k) + Z_l(k), \tag{8}$$

Considering that $T_{cp} \geq \tau_{max}$, where, T_{cp} is the cyclic prefix interval time, τ_{max} corresponds to the maximum excess delay from a generic multipath channel, k denotes the subcarrier frequency component of the l^{th} transmitted OFDM signal, $H_l(k)$ is the Channel Frequency Response (CFR) and $Z_l(k)$ is the AWGN in the frequency domain. The original transmitted information, $X_l(k)$ can be recovered employing a Frequency Domain Equalization (FDE) technique [25], which is performed as a K-branch linear feed-forward equalizer with $C(k)$ being the complex coefficient of the k^{th} subcarrier. Minimum Mean Square Error (MMSE) equalizer is considered, where for this criterion, $C(k)$ is defined by (9).

$$C_{MMSE}(k) = \frac{\hat{H}(k)^*}{|\hat{H}(k)|^2 + \frac{1}{\eta}} \tag{9}$$

where, $\hat{H}(k)$, η, * and $|.|$ denote the estimated CFR, SNR, conjugate transpose and modulus, respectively.

FEC schemes should be determined considering the trade-off between higher coding gain, hardware complexity and code rate. Two families of linear block codes are proposed in the standard: RS codes (mandatory) and LDPC codes

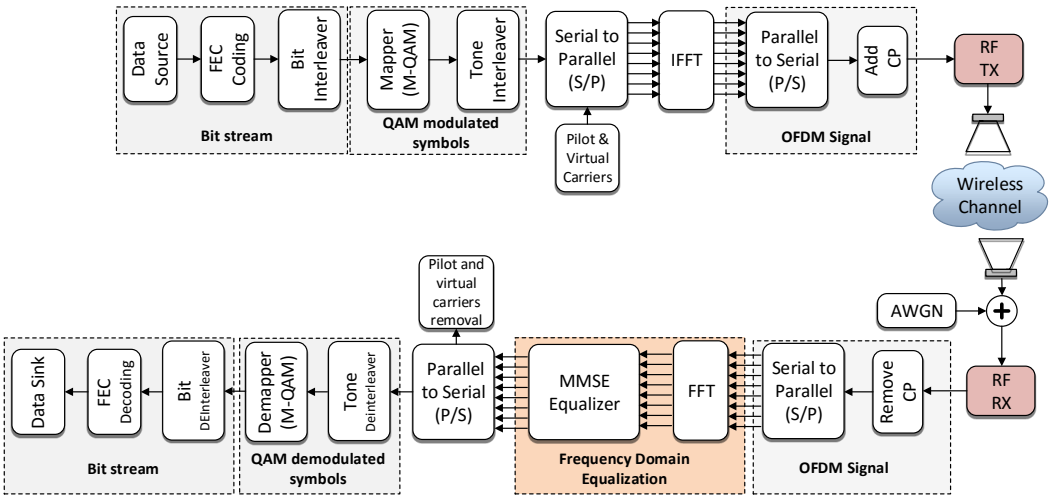

Figure 3: OFDM block diagram.

(optional) with several coding rates. RS codes are known for their good capability of burst error correction at a relatively high SNR. LDPC codes, despite having high complexity, with its iterative decoding process, ensures a better error correction performance than Reed Solomon codes or turbo codes [26] and its performance is very close to the Shannon coding limit [27].

4. Effect of RF and Channel impairments on OFDM performance

Non-linearities in wireless systems mainly result in performance degradation. The response of non-linear systems are, usually characterized by undesirable signal components in addition to the desired signal. Therefore, this section presents a study of performance degradation due to the inclusion of individual RF impairments on the uncoded OFDM, namely, PN, IQ imbalances and power amplifier non-linearities. The effect of the RF impairments, is implemented based on the models introduced in section 2. This is achieved through BER analysis for 16 and 64 QAM, under an AWGN channel. The considered BER target, recommended for video streaming applications is 10^{-6} [2].

4.1. Phase Noise and IQ imbalances

The impact of phase noise on the performance of OFDM using 16 QAM (Fig. 4a) and 64 QAM (Fig. 4b), for four low frequency PN constants: -87, -90, -93 and -96 dBc/Hz [17], where -87 and -96 represent the worst and best case scenarios, respectively. It can be clearly seen that the presence of PN degrades the overall system performance, requiring larger E_b/N_0 values to achieve a desired BER. i.e for the worst case scenario (PSD (0) = -87 dBc/Hz), the degradation of the OFDM performance is about 1.5 dB for 16 QAM, while in the 64 QAM system, the BER target is not achievable.

The effect of IQ imbalances on BER analysis depends on the type of IQ mixers and the number of upconversion/downconversion stages present in the RF front-end architecture. The phase gain mismatch (Δg) and phase mismatch ($\Delta\theta$) values vary from 0 to 0.5 dB and from 0 to 6 degrees, respectively [17]. Figures 4c and 4d demonstrate the effect of IQ imbalances considering both modulation orders, where the OFDM system employing 16 QAM is slightly more robust against IQ imbalances than 64 QAM (to achieve the required BER of 10^{-6}). 16 QAM requires approximately 8.5 dB lower value of E_b/N_0 for the worst case scenario (Δg = 0.5 dB and $\Delta\theta = 6^{\circ}$), in comparison with the 64 QAM.

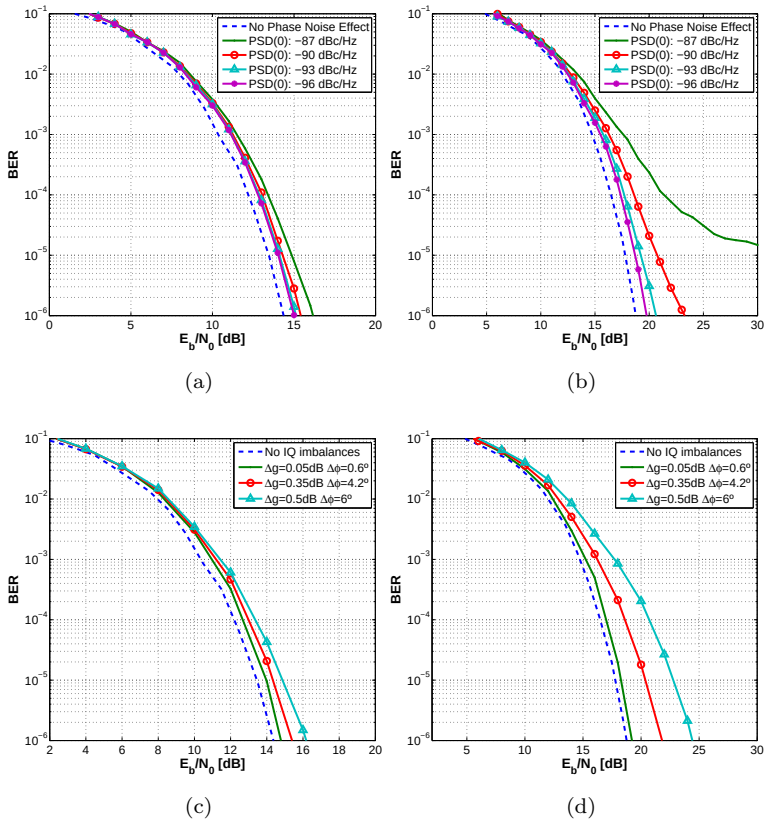

Figure 4: BER performance under PN and IQ imbalances effect, respectively, for (a) (c) 16 QAM, and (b) (d), 64 QAM.

4.2. Power Amplifier

The effects of the in-band and out of band distortions, due to the non-linear PA response, modelled in section 2.2 for uncoded OFDM, are presented in this section. The out of band emissions do not have a direct impact on the system performance, but may harm communication systems operating in the adjacent frequency channels. Nevertheless in-band emissions introduce ISI. In order to minimize the effect of out of band emissions, the spectrum of the transmitted signal must be below the Transmit Spectrum Mask (TSM) is defined by the IEEE 802.15.3c standard [1]. The estimation of such spectrum was performed by calculating the transmitted Signal Power Spectrum Density (PSD).

Table 3: OBO required to meet TSM requirements for 60 GHz OFDM systems.

PA model	**Modulation**	**PD**	**OBO [dB]**	η [%]
GaAs	16 QAM	yes	5.5	19.95
		no	9.2	8.25
	64 QAM	yes	6	17.78
		no	9.5	7.7
CMOS	16 QAM	yes	5.5	12.56
		no	9.5	4.58
	64 QAM	yes	5.9	11.45
		no	9.6	4.48

The transmitted OFDM signal amplitude might exhibit high peak values, since many subcarrier components are added in the IFFT operation. However, a discrete representation of the OFDM signal does not necessarily contain the maximum amplitude values of the continuous time domain signal. Therefore, an oversampled version of the discrete signal is considered, yielding a more accurate PAPR distribution of the OFDM signals. An oversampling factor of L = 4 is considered for both QAM modulations.

The PSD has been computed for both PA technologies. Estimated OBO values for both PA models and both modulations are summarized in Table 3, and illustrated, in particular for 16 QAM, in Fig. 5a and in Fig. 5b without and with PD, respectively. Results show that the minimum estimated OBO values, which meet the TSM requirements are slightly higher for 64 QAM, as expected. The PAPR distribution employing 64 QAM has slightly higher values than 16 QAM. In addition, introducing a PD technique reduces the OBO values for both amplifier technologies and consequently increases their power efficiency, e.g. for the GaAs model the PAE increases from 8.25% to 19.95% (16 QAM). Furthermore, both PA models present similar OBO values to meet the TSM requirements. i.e., for the GaAs model using PD, the lowest values of PA OBO are 5.5 and 6 dB for both modulation schemes, whereas the CMOS model requires OBO values of 5.5 and 5.9 dB, respectively.

Table 4: Summary of PA non-linearity impact on BER results for 60 GHz OFDM systems.

PA model	**M-ary**	**PD**	E_b/N_0 **[dB]**	$\triangle E_b/N_o$ **[dB]**	**OBO [dB]**	η **%**
GaAs	16	yes	20.5	6.1	6	17.7
		no	26	11.6	9	8.6
	64	yes	26.2	7.45	8	11.2
		no	32	13.25	13	3.44
CMOS	16	yes	23.7	9.3	7	8.89
		no	21.6	7.2	11	3.26
	64	yes	28.65	9.9	12	2.81
		no	26	7.25	15	1.3

A summary of PA non-linearity impact on BER results against PA OBO for both PA models, is presented in Table 4. In this table, the performance degradation is characterized by $\triangle E_b/N_o$, which is the difference between the required E_b/N_0 in the presence and absence of non-linearities. Simulated results have shown that the PA OBO has a significant impact on the BER performance. A trade-off is noticed between the PA operating point, $\triangle E_b/N_o$ and PAE, i.e, in order to mitigate the effects of the PA non-linearities on the system, the power efficiency of the PA is significantly decreased. Pre-distortion employment allows to reduce the signal degradation for lower PA OBO values, making the system more power efficient and more robust against this impairment, as demonstrated with the comparison between Fig. 5c and Fig. 5d.

Additionally, when comparing the BER simulation results for both PAs, it is noticed that the GaAs PA is a better choice for the RF front-end, as it is capable to achieve the desirable BER target with lower PA OBO values at a higher power efficiency. The system requires 6 and 8 dB of PA OBO (optimum values) using GaAs model and PD for 16 and 64 QAM, respectively. On the other hand, the CMOS model requires 7 and 12 dB for 16 and 64 QAM, respectively. This can be justified by the fact that CMOS PA model is being characterized by a high phase distortion on its AM-PM curve, as is evident in Fig. 2c.

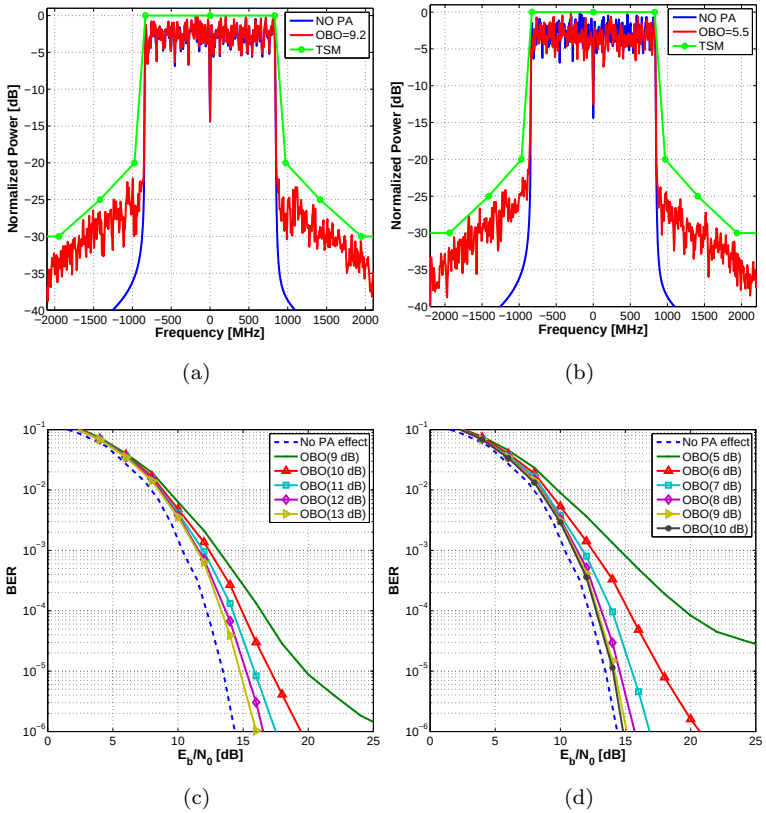

Figure 5: (a) (b) estimated OOBEs and (c) (d) OFDM BER performance employing GaAs PA without and with PD for 16 QAM.

4.3. Effects of Channel Impairments

In this section, the uncoded OFDM system performance over the IEEE CM9 standard model [2] (typical indoor LOS kiosk environment) at 60 GHz is assessed using MMSE equalization and employing both QAM modulations. Moreover, the maximum separation between terminals as a function of E_b/N_0 is also obtained.

The complex Channel Impulse Response (CIR) for the CM9 channel is obtained from an IEEE statistical model [28], which takes into account the variation of the T_X and R_X antenna heights and the scatterers position in the multipath environment, following a random quasi-static channel distribution.

Based on the suggested Equivalent Isotropically Radiated Power (EIRP) of 40 dB [22] and a receiver gain antenna (G_{RX}) of 10 dBi (typical value of gain on-chip antennas at 60 GHz) [29], the dynamic range of the average PDP is computed considering all multipath components which are 10 dB above the noise floor (-81.4 dBm), considering a channel bandwidth of 1.815 GHz. Consequently, the PDP has been analysed in terms of averaged RMS delay spread ($\bar{\tau}_{RMS}$), coherence bandwidth for signals correlation of 0.9 ($\bar{B}_{c_{0.9}}$) and Rician factor ($\bar{K}$). Results are as follows: $\bar{\tau}_{RMS} = 2.9\ ns$, $\bar{B}_{c_{0.9}} = 258.1\ MHz$ and $\bar{K} = 52.62\ dB$. Moreover, the considered Half Power Beamwidth (HPBW) of T_X/R_X antennas is 30° and 30°, respectively.

The BER performance of OFDM over the CM9 channel is depicted in Fig. 6. From the results it is possible to conclude that BER curves varies from one channel realization to another, since each CIR is characterised with different statistical values of τ_{RMS}, K, and $B_{c_{0.9}}$. Due to the statistical nature of the model [28], it is expected that BER curves converge with the increase of the number of iterations. Therefore, 100 realizations were considered in this work respecting a relatively good commitment between simulation time and accuracy.

In order to assess the effect of the kiosk multipath environment on the OFDM system, the average of BER performance is conducted. With this, it is verified that 16 QAM uncoded OFDM BER performance is similar to that obtained with AWGN. This is explained by the fact the former is characterized by a very high Rician factor and a relatively high coherence bandwidth. Whereas, the performance of the 64 QAM uncoded OFDM system is inferior rendering it to be inoperable for BER below 10^{-6}.

The maximum separation between terminals (d_{max}) as a function of E_b/N_0 has been estimated, based on the relation between the maximum operation range, d_{max}, and the link-budget equation, given by (10) [30] and (11), respectively.

$$d_{max} = 10^{(PL-PL_o)/10n}\ [m], \tag{10}$$

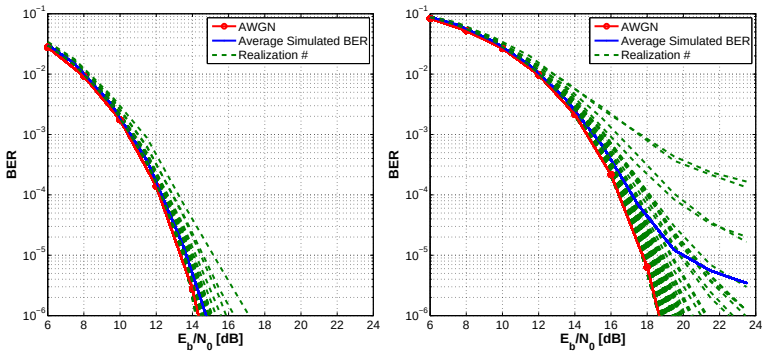

(a) (b)

Figure 6: Average BER for the considered fading channel for: a) 16 QAM b) 64 QAM.

$$PL = EIRP + G_{RX} - P_N - E_b/N_o - IL - M \ [dB], \tag{11}$$

where, PL_0 is the path loss at $d_0 = 1m$, n is the path loss exponent and PL is the path loss. Values of $n = 2$, $PL_0 = 68$ dB reported by the TG3c group [2]. In (11), P_N is the average noise power per bit, where $P_N = N + N_f$ and $N = -174 + 10log_{10}(throughput\ [bps])$, N_f is the receiver noise figure, IL is the implementation loss of the transceiver and M the link margin. In addition, $N_f = 8$ dB, $IL = 2$ dB and $M = 5$ dB can be found in [31] for a 60 GHz transceiver.

5. Impact of RF front-end non-linearities at 60 GHz

In this section, the effect of RF impairments on the quality of uncompressed wireless video streaming for UM1 application, defined by standard [4], is evaluated and demonstrated under different impairment conditions (case studies) over CM9 channel. Hence, it is possible to accurately estimate the impact of a realistic RF front-end on a wireless mmWave OFDM (uncoded and coded) communication system, under various scenarios for a combination of optimum and non-optimum non-linearity values based on results presented in section 4.2.

Table 5: Relation between subjective and objective quality indicators.

PSNR [dB]	**ITU Quality scale**
> 37	5 - Excellent
$31 - 37$	4 - Good
$25 - 31$	3 - Satisfactory
$20 - 25$	2 - Poor
< 20	1 - Very poor

Therefore, five distinct case studies (A to E) have been built based on a combination of different QAM modulation order, PA OBO values, IQ imbalances and PSD(0) modelling values. Those are thoroughly reported in Table 6.

The quality of the transmitted uncompressed video content, in Full HD, is assessed through BER and PSNR analysis. Moreover, it is possible to estimate the minimum value of E_b/N_0 to ensure a relatively good subjective quality considering a reference video frame. This is achieved by using the relation between the PSNR (objective quality assessment metric) and the subjective quality assessment based on viewer's impression, presented in Table 5 [32].

Table 6: Case study RF impairments values.

Case studies	**M-ary**	**PA OBO [dB]**	**IQ (Δg [dB], $\triangle\theta$ [°])**	**PSD(0) [dBc/Hz]**
A	16	6	(0.05,0.6)	-96
	64	8		
B	16	6	(0.5,6)	-96
	64	8		
C	16	6	(0.05,0.6)	-87
	64	8		
D	16	6	(0.5,6)	-87
	64	8		
E	16	5.5	(0.5,6)	-87
	64	6		

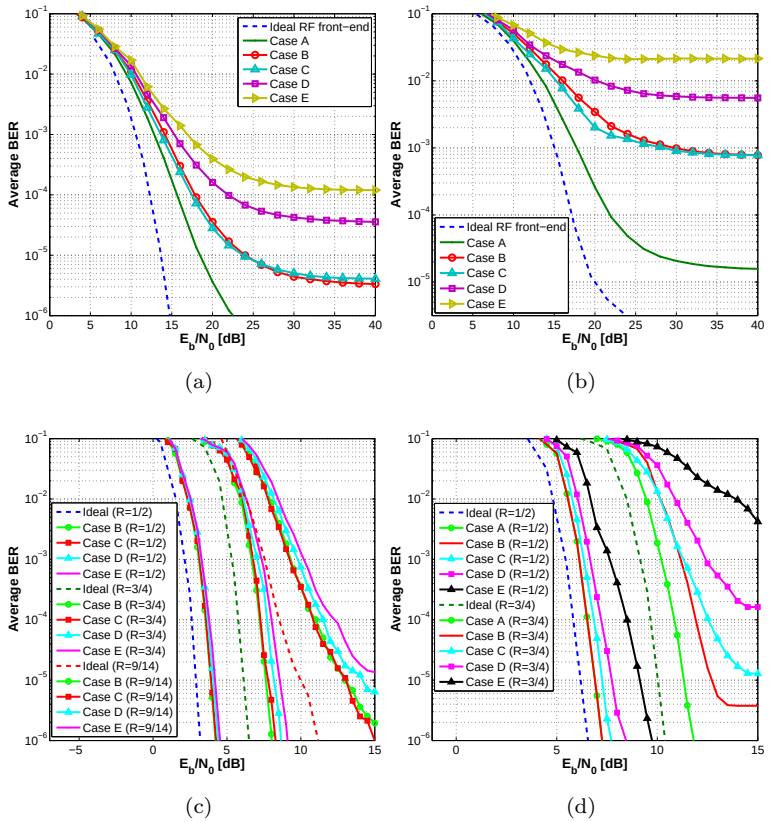

Figure 7: BER performance for various case studies: uncoded OFDM for a) 16 QAM b) 64 QAM and Coded OFDM for c) 16 QAM and d) 64 QAM modulations.

The uncoded OFDM BER results, computed for each case study, are displayed in both Fig. 7a and Fig. 7b, for 16 QAM and 64 QAM, respectively, where "Ideal RF front-end" means that only the effect of the multipath propagation is taking into account. It is evident from these results that the desired BER is only achievable using 16 QAM for case study A, which corresponds to a maximum system range of 10.2 m, according to (10). In order to minimize ISI, in particular, in cases where the BER target is not achieved and consequently increasing operation range, FEC code schemes RS(224,216), LDPC(672,336) and LDPC(672,504) with coding rates of 9/14, 1/2 and 3/4, respectively, are considered.

Table 7: Summary of RF front-end non-linearity impact on the BER results for 60 GHz coded OFDM systems for 16 QAM.

Case Studies	**Coding**	E_b/N_0 [dB]	$\triangle E_b/N_o$	d_{max} **[m])**
B	R=3/4	8	1.51	73.7
	R=9/14	15	4	35.6
C	R=3/4	8.1	1.6	72
	R=9/14	-	-	-
D	R=1/2	4.05	1.05	143.1
	R=3/4	8.6	2.1	68.8
	R=9/14	-	-	-
E	R=1/2	4.15	1.15	139.7
	R=3/4	9.1	2.6	64.1
	R=9/14	-	-	-

In Fig. 7c and Fig. 7d, it is clearly shown that the C-OFDM outperforms the uncoded OFDM under both RF and channel impairments, but at the expense of system throughput. Moreover, as expected the LDPC coding with its iterative decoding and exploitation of frequency diversity leads to impressive results. For example, using RS FEC coding, 16 QAM OFDM BER performance fails to meet the BER target for C, D and E case scenarios. However, for the 64 QAM system with LDPC (672,504), the BER target is only achieved for case study A, whereas, the 16 QAM OFDM system is able to achieve the BER target in all case scenarios, making the wide-band wireless transmission reliable regardless of the impact of non-linearities. A summary of RF front-end non-linearity impact over CM9 channel on the BER results and maximum range for 60 GHz coded OFDM systems, using 16 and 64 QAM, are shown in Table 7 and Table 8, respectively.

In order to evaluate the effectiveness of uncoded OFDM in ensuring a good Quality of Service (QoS), at appropriate PSNR values, the degradation of the quality of the video frame for the best case scenario (case A), has been studied. The video frame content (Fig. 8a) is divided into several transmitting OFDM

Table 8: Summary of RF front-end non-linearity impact on the BER results for 60 GHz coded OFDM systems for 64 QAM.

Case Studies	**Coding**	E_b/N_0 **[dB]**	$\triangle E_b/N_o$	d_{max} **[m])**
A	R=1/2	7.1	1.1	82.6
	R=3/4	12	2	38
C	R=1/2	7.5	1.45	79.1
D	R=1/2	8.2	2.2	72.1
E	R=1/2	9.6	3.6	61.3

symbols and then transmitted over the channel model. PSNR results are depicted in Fig. 8c, for both modulation schemes together with those obtained for an ideal RF front-end, where dash curves show the BER results over AWGN. It be can seen that both RF and channel impairments have significant impact on the degradation of the quality of reference video frame,where the presence of distorted pixels is clearly visible when compared to those of Fig. 8a and Fig. 8b, and a maximum achievable PSNR of about 24 dB (for an $E_b/N_o = 24$ dB) for both modulations. This characterizes the video frame subjective quality as poor (Table 5), while the effective objective quality degradation ($\triangle PSNR$), which is the difference between the PSNR in absence and presence of non-linearities to achieve an excellent video quality, is about 17 dB for same E_b/N_0. Therefore, in order to ensure reliable QoS ($PSNR > 31$) and consequently reducing the necessary SNR to meet this quality requirement, FEC schemes are selected based on their BER performance, complexity and system throughput. Based on results presented in Fig.7 for the worst case scenarios, i.e case study D and E, 16 QAM RS (224,216) lend itself to be the preferred option, since 64 QAM requires LDPC (672,336). Although both modulation schemes operate approximately at the same throughput rate, LDPC (672,336) increases significantly the overall system complexity in comparison with RS (224,214). The 16 QAM C-OFDM system ensures an excellent and satisfactory QoS under the worst case scenarios (D and E) with $E_b/N_o = 24$, as demonstrated in Fig. 8d, which restricts the maximum distance between T_X/R_X to 12.62 m. In other words, for a satis-

factory QoS the streaming video device and a TV/projector or other receiver equipment should be at a distance smaller than 12.62 m.

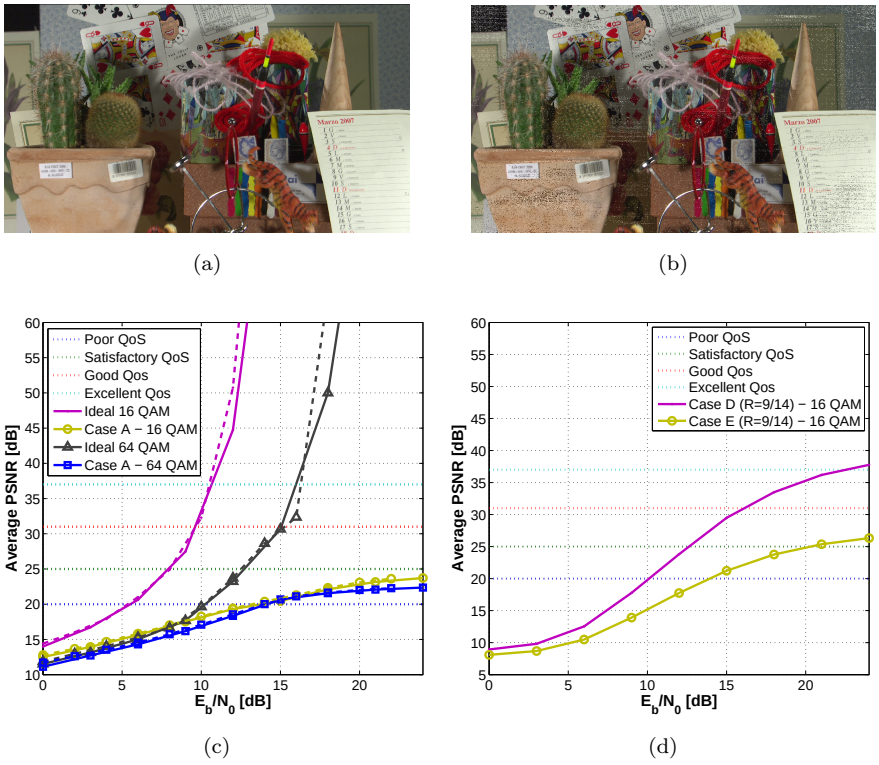

Figure 8: Subjective video quality performance assessment of the received video frame for an "Ideal RF front-end" a) and under impairments b) for an $E_b/N_o = 24$ dB using 16 QAM. In c) and d) the impact of impairments on the objective quality of the received frame vs E_b/N_0 is conducted for uncoded and coded OFDM, respectively.

6. Conclusions

In this paper, a study of the impact of RF impairments on a 60 GHz OFDM (uncoded and coded) system, implemented according to the IEEE 802.15.3c standard, for high data-rate applications, and considering 16 QAM and 64 QAM, was presented. Degradation in system performance due to phase noise char-

acteristics, IQ imbalances and power amplifier non-linearities, was evaluated. Such impairments were modelled and used to characterize a realistic generic RF front-end system. The performance assessment of the OFDM system was conducted through BER and PSNR analysis considering the transmission of an uncompressed Full HD video frame over an AWGN radio channel model.

It has been shown that PA non-linearities induce the largest performance degradation in the OFDM system, when compared with PN and IQ imbalances. This limitation has been compensated for by the introduction of a PA PD technique, which allows to achieve a good communication quality, reducing the required PA OBO value which, however, remains above those of 6 dB and 8 dB estimated using a GaAs PA for 16 QAM and 64 QAM, respectively. It is concluded that, in order to decrease further these values, a PAPR reduction technique should be considered in the system design, together with PD. This is particularly important if a mobile equipment is used as either TX or RX, since the efficiency of PA should be as high as possible to overcome battery saving requirements.

It is also concluded that the modulation order is important in OFDM system design, in particular at high frequencies and in uncoded systems, since high order modulations present higher sensitivity to bit errors in presence of impairments. For example, it has been shown that for channels with small time dispersion characteristics such as the CM9, BER values of 10^{-6} cannot be achieved for 64 QAM OFDM without FEC schemes. Whereas a performance similar to that of AWGN is noted for uncoded 16 QAM system. This makes the system performance impractical in some cases. For example, 64 QAM with coded OFDM, which enhance the spectral efficiency of the system, just ensures a reliable wireless communication system for worst case scenarios considering LDPC (672,336) coding. This makes the system to operate at approximately the same rate as the 16 QAM with RS (224,216), but with higher complexity.

Additionally, it is concluded that a coded 16 QAM OFDM system operating under RF and channel impairments is robust enough to provide a relatively good quality of service in streaming uncompressed video for wireless applications, for

a range shorter than 13 m. Hence, PN, IQ imbalances and PA non-linearities have direct impact on the potential OFDM system throughput. Both uncoded 16-QAM and 64-QAM OFDM systems fail to achieve the required performance target (for all RF impairment combinations), and coded 64-QAM systems require large coding rates.

Finally, results presented in this work provide an important guidance for 60 GHz OFDM system design principles, in particular for uncompressed wireless video streaming applications.

References

[1] 802.15.3c-2009 - Physical Layer (PHY) Specifications for High Rate Wireless Personal Area Networks(WPANs).

[2] S.-K. Yong, TG3c Channel Modeling Sub-committee Final Report, Samsung Advanced Institute of Technology, 2007.

[3] T. Baykas et al, Ieee 802.15.3c: the first ieee wireless standard for data rates over 1 gb /s 49.

[4] A. Sadri, Summary of the Usage models for 802.15.3c, 2006.

[5] H. Yang, P. F. M. Smulders, M. H. A. J. Herben, Channel characteristics and transmission performance for various channel configurations at 60 ghz, EURASIP J. Wirel. Commun. Netw. 2007 (2007) 43–43.

[6] J. Nsenga, W. V. Thillo, F. Horlin, A. Bourdoux, R. Lauwereins, Comparison of oqpsk and cpm for communications at 60 ghz with a nonideal front end, EURASIP Journal on Wireless Communications and Networking 2007 (2007) 086206.

[7] N. Guo, R. C. Qiu, S. S. Mo, K. Takahashi, 60- ghz millimeter - wave radio : Principle , technology , and new results, EURASIP Journal on Wireless Communications and Networking 2007 (2006) 068253.

[8] H. Mehrpouyan et al, Improving bandwidth efficiency in e-band communication systems, IEEE Communications Magazine 52 (3) (2014) 121–128.

[9] M. Lei et al, Hardware impairments on ldpc coded sc - fde and ofdm in multi - gbps wpan (ieee 802.15.3c), 2008.

[10] A. Maltsev, A. Lomayev, A. Khoryaev, A. Sevastyanov, R. Maslennikov, Comparison of power amplifier non - linearity impact on 60 ghz single carrier and ofdm systems, 2010.

[11] H. Yang, P. Smulders, E. Fledderus, Comparison of single - and multi - carrier block transmissions under the effect of nonlinear hpa, 2007.

[12] U. Rizvi, G. Janssen, J. Weber, Impact of rf impairments on the performance of multi -carrier and single -carrier based 60 ghz transceivers, 2007.

[13] F. Horlin, A. Bourdoux, Comparison of the sensitivity of ofdm and sc - fde to cfo , sco and iq imbalance, 2008.

[14] Y. Zou et al, Impact of major rf impairments on mm- wave communications using ofdm waveforms, 2016, pp. 1–7.

[15] A. A. A. Boulogeorgos et al, Effects of rf impairments in communications over cascaded fading channels, IEEE Transactions on Vehicular Technology 65 (11) (2016) 8878–8894.

[16] Y. Shoji et al, Rf impairment models for 60 ghz -band sys / phy simulation (nov 2006).

[17] V. Erceg et al, 60 ghz impairments modeling (nov 2009).

[18] N. Y. Ermolova, Y. Zou, M. Valkama, O. Tirkkonen, Error-rate analysis of ofdm radio link over mobile rayleigh channel under multiple rf impairments, IEEE Transactions on Vehicular Technology 63 (2) (2014) 930–936.

[19] R. Gomes et al, Performance and evaluation of ofdm and sc - fde over an awgn propagation channel under rf impairments using simulink at 60 ghz, 2014.

[20] J. Andrews, S. Buzzi, W. Choi, S. Hanly, A. Lozano, A. Soong, J. Zhang, What will 5g be?, Selected Areas in Communications, IEEE Journal on 32 (6) (2014) 1065–1082.

[21] D. Soldani, A. Manzalini, Horizon 2020 and beyond: On the 5g operating system for a true digital society, IEEE Vehicular Technology Magazine 10 (1) (2015) 32–42.

[22] S. Yong, P. Xia, A. Garcia, 60GHz Technology for Gbps WLAN and WPAN : From Theory to Practice, Wiley Publishing, 2011.

[23] C. Rapp, Effects of hpa -nonlinearity on a 4- dpsk / ofdm -signal for a digital sound broadcasting system.

[24] M. Varonen, M. Karkkainen, K. Halonen, Millimeter-wave amplifiers in 65-nm cmos, 2007.

[25] M. Lei, I. Lakkis, H. Harada, S. Kato, Mmse - fde based on estimated snr for single - carrier block transmission (scbt) in multi - gbps wpan (ieee 802.15.3c), 2008.

[26] N. Bonello, S. Chen, L. Hanzo, Design of low-density parity-check codes: An overview, IEEE VechicularTechnology Magazine (2011) 16–23.

[27] C. Shannon, A mathematical theory of communication, Bell System Technical Journal, The 27 (1948) 379–423 ,.

[28] H. Harada et al, CM MATLAB Release Support Document, 2007.

[29] R. Daniels, J. Murdock, T. Rappaport, R. Heath, 60 ghz wireless: Up close and personal, IEEE Microwave Magazine 11.

[30] T. Baykas et al, Operation range estimation of reed - solomon coded sc - fde system in 60- ghz wpans, Vol. 1, 2008.

[31] S. Alireza, Philips, TG3C Selection Criteria, 2007.

[32] H. K. Kim et al, IAENG Transactions on Engineering Technologies : Special Edition of the World Congress on Engineering and Computer Science 2011, Springer Science & Business Media, 2012.